

Supporting Information

3D-honeycomb-like catalyst: nitrogen-doped carbon material with cobalt and manganese-oxide for the C-H bond oxidation

**Kaizhi Wang^{&a}, Shiling Zhao^{&b}, Lei Ma^a, Ming Yang^a, Jiaheng Qin^a, Xiaokang Huang^a, Li Gong^a, Yucong Xiong^a,
and Rong Li^{*a}**

& These authors contributed equally to this work should be considered co-first authors.

^a State Key Laboratory of Applied Organic Chemistry (SKLAOC), College of Chemistry and Chemical Engineering, Lanzhou University, Lanzhou 730000, PR China.

^b Laboratory of Mesoscopic Chemistry, College of Chemistry and Chemical Engineering, Nanjing University, Nanjing 210023, PR China.

E-mail: liyirong@lzu.edu.cn; Fax: +86-931-891-2582; Tel: +86-18919803060

Table of Contents

1. Synthesis of the comparative pre-catalysts of 3D-honeycomb-like	S3
2. Pre-catalyst Characterization	S3
3. Supplementary Table	S5
Table S1 Comparative chart of catalytic activity of Co-MnO@CN-700-m:n in ethylbenzene to acetophenone reaction.	S5
Table S2 XPS analysis, ICP-OES, and element content for pre-catalysts.....	S5
Table S3 Comparative chart of catalytic activity of Co-MnO@CN-700 with other reported catalysts.....	S6
4. Supplementary Figures	S7
Fig. S1 SEM images of Co-MnO@CN-180 (a), Co-MnO@CN-500 (b), Co-MnO@CN-600 (c), Co-MnO@CN-800 (d), Co-MnO@SiO2-700 (e), Co-MnO@SBA-15-700 (f), Co-MnO@CNTs-700 (g), and Co-MnO@AC-700 (h)	S7
Fig. S2 HRTEM image (a), selected-area diffraction image (b), HAADF-STEM image (c), mapping images of the Co and Mn elements (d), EDS image (e) and line scanning image (f) of Co-MnO@CN-700.....	S7
Fig. S3 Comparison of XRD patterns with those of previously reported materials.....	S8
Fig. S4 Comparison of Raman spectra with those of previously reported materials	S8
Fig. S5 Comparison of nitrogen adsorption-desorption isotherms with those of previously reported materials.....	S9
Fig. S6 H ₂ -TPR results of as-prepared catalysts.....	S9
Fig. S7 Comparison of FT-IR spectra with those of previously reported materials	S10
Fig. S8 XRD pattern of reused material.	S10
Fig. S9 SEM images of reused material.....	S11
Fig. S10 The wide-scan XPS of material adsorbed with TBHP and ethylbenzene.	S11
References.....	S12

1. Synthesis of the comparative pre-catalysts of 3D-honeycomb-like

The synthesis of 3D-honeycomb pre-catalyst involves two simultaneous reactions. In the first step, polyacrylonitrile, cobalt acetate tetrahydrate, manganese acetate tetrahydrate and DMF (15 mL), which is called the mixture solution 1 (M1), are drastically stirred in a 25 mL round-bottomed flask by magnetic stirrers at 60 °C for 1 h. Simultaneously, glycerol (10 mL) and isopropanol (45 mL), which is called the mixture solution 2 (M2), are adding in a 100mL two-neck round bottom flask. The M2 is vigorously stirred by mechanical stirring at 1000 rpm for 1 h under ice bath conditions. In the second step, after reacting for 1 hour, M1 should be added to M2 quickly and drop by drop, and stirring is continued for 0.5 h while maintaining at the same stirring rate under the same temperature conditions. Then, a heterogeneous precursor mixture solution is acquired, and then the mixture solution is collected into a 100 mL stainless steel teflon autoclave and kept in a sealed oven at 180 °C for 6 h. When it cooling down unaffectedly, the pink particles are collected by centrifugation and followed by drying in a vacuum oven at 80 °C for 12 h, and it is named as Co-MnO@CN-180. Later, the dried mixture precursor particles passed through a heating zone at 300 °C for 2 h carbonized at 700 °C for 120 min each, under N₂ atmosphere at a heating rate of 2 °C/min. the synthesis other contrastive 3D-honeycomb-like pre-catalysts are shown in Table S1, where exhibits all procedures remain unchanged except for the Co/Mn mass ratio (Co : Mn = 2:0; 3:1; 2:1; 1:2; 1:3; 0:2), they are called Co-MnO@CN-700-m:n (m:n represents the Co/Mn mass ratio).

2. Pre-catalyst Characterization

The XRD pattern of the pre-catalysts were recorded by X-ray diffractometer (XRD) Rigaku D/max-2400 and the radiation is Cu-K α ($\lambda=1.5406 \text{ \AA}$). The size of the crystallite is evaluated by the Schere's formula ($D_{XRD} = K\lambda/\beta\cos\theta$), β is observed angular width at half maximum intensity of the peak, K is a dimension less number, λ is the x-ray wavelength (1.5418 \AA for

Cu $K\alpha$) and θ is the diffraction angle. Meanwhile, the experimental XRD pattern is compared with joint committee on powder diffraction standards (JCPDS) to obtain the phase composition of the material. The metal content was measured by Inductive Coupled Plasma Optical Emission Spectrometer (ICP-OES), which is carried out with Perkin Elmer (Optima-4300DV). Scanning electron microscopy (SEM) was recorded on MIRA3 TESCAN instrument. The transmission electron microscopy (TEM), high-resolution transmission electron microscopy (HR-TEM) and EDX were operated on Tecnai G2Tf20 with a field gun operating at 300 kV. The specimens were dispersed in ethanol and on a holed carbon-coated Cu grid. Nitrogen physisorption isotherms were carried out at $-195.8\text{ }^{\circ}\text{C}$ on a static volumetric instrument (TriStar II 3020 V1.04). The specific surface area is calculated by the Brunauer–Emmett–Teller method. X-ray photoelectron spectroscopy (XPS) was performed on the PHI-5702 instruments with an Mg anode (Mg $K\alpha$ $h\nu = 1253.6\text{ eV}$) at a base pressure of 5×10^{-8} mbar). The revision of the binding energies (BE) is implemented with the C 1s peak of extraneous C at 284.6 eV. Nitrogen physisorption isotherms were carried out the pore size distribution and pore volume on a static volumetric instrument (TriStar II 3020 V 1.04). The specific surface area was analyzed by the Brunauer-Emmett-Teller (BET) method. Fourier transform infrared spectroscopy (FT-IR) spectra were obtained on a Bruker spectrometer (VERTEX 70). Elemental analysis (EA, CHNS) was detected the content of C, H, and N elements in pre-catalysts. Thermogravimetric analysis (TGA, TA-Q50) measured the mass change of N-doped carbon material, heated from 25 to $800\text{ }^{\circ}\text{C}$ under N_2 atmosphere at a heating rate of $2\text{ }^{\circ}\text{C min}^{-1}$.

3. Supplementary Table

Table S1 Comparative chart of catalytic activity of Co-MnO@CN-700-m:n in ethylbenzene to acetophenone reaction.^a

Catalysts/mg	Raw material addition amount			Time (h)	Conv. (%)	Sel. (%)
	PAN/g	Co/g	Mn/g			
Co-MnO@CN-700/15	1.05	0.25	0.25	6	99.9	99.9
Co-MnO@CN-700-2:0/15	1.3	0.25	0	6	62	86
Co-MnO@CN-700-3:1/15	1.25	0.25	0.1	6	73	94
Co-MnO@CN-700-2:1/15	1.15	0.25	0.15	6	81	89
Co-MnO@CN-700-1:2/15	1.15	0.15	0.25	6	95	91
Co-MnO@CN-700-1:3/15	1.25	0.1	0.25	6	98	87
Co-MnO@CN-700-0:2/15	1.3	0	0.25	6	98	73

^a Reaction conditions: 1 mmol EB, 15 mg pre-catalyst, 0.5 mL TBHP and 5 mL deionized water are added in the reaction system. The conversion and selectivity are tested by GC-MS.

Table S2 XPS analysis, ICP-OES, and element content for pre-catalysts.

Sample	XPS analysis					ICP-OES		EA		
	Co (at. %)	Mn (at. %)	C (at. %)	N (at. %)	O (at. %)	Co (wt. %)	Mn (wt. %)	C (wt. %)	N (wt. %)	O (wt. %)
Co-MnO@CN-180	-	-	-	-	-	3.41	3.26	36.58	10.76	2.97
Co-MnO@CN-500	2.59	3.63	75.68	4.70	13.40	7.15	6.98	48.43	8.19	1.51
Co-MnO@CN-600	-	-	-	-	-	7.47	7.09	49.26	7.49	0.92
Co-MnO@CN-700	3.23	3.59	78.86	2.68	11.64	8.12	7.26	62.33	2.78	0.52
Co-MnO@CN-700-Reused	-	-	-	-	-	7.28	6.78	57.81	2.58	0.29
Co-MnO@CN-800	-	-	-	-	-	9.88	9.32	67.57	1.09	0.13

Table S3 Comparative chart of catalytic activity of Co-MnO@CN-700 with other reported catalysts.

Catalysts/mg	Temp. (°C)	Time (h)	Oxidant /(mmol)	Solvent /(mL)	Conv. (%)	Sel. (%)	Ref.
Co-MnO@CN-700/15	50	6	TBHP/3.5	Water/5	99.9	99.9	This work
Ti-Zr-Co /10	160	3	O ₂ (2 MPa)	CH ₃ CN ₂ /5	61.9	69.2	[1]
Mn-SiO ₂ -Al ₂ O ₃ /50	80	24	TBHP/2	-	68	93	[2]
Fe-SiO ₂ -Al ₂ O ₃ /50	50	24	TBHP/9	-	80	99.9	[3]
Fe ₃ O ₄ -MnCP@SiO ₂ /100	100	10	O ₂ (1 atm)	-	15	22	[4]
5 mol % CoBr ₂	120	0.1	Air (12 bar)	AcOH	80	84	[5]
MgCuAl/200	130	12	TBHP/20	-	80	92	[6]
Cr cation sites/500	130	24	O ₂	-	48	-	[7]
Mn-SiO ₂ -Al ₂ O ₃ /50	120	8	TBHP/2	-	84	86	[8]
SNC-Ca-850/10	80	4	TBHP/2	Water/5	92	97	[9]
Co clusters solution/3mL	100	50	O ₂	n-decane /1.2	51	31	[10]
Mn(TMCP)/50	150	6	TBHP/9.3	-	48	96	[11]

4. Supplementary Figures

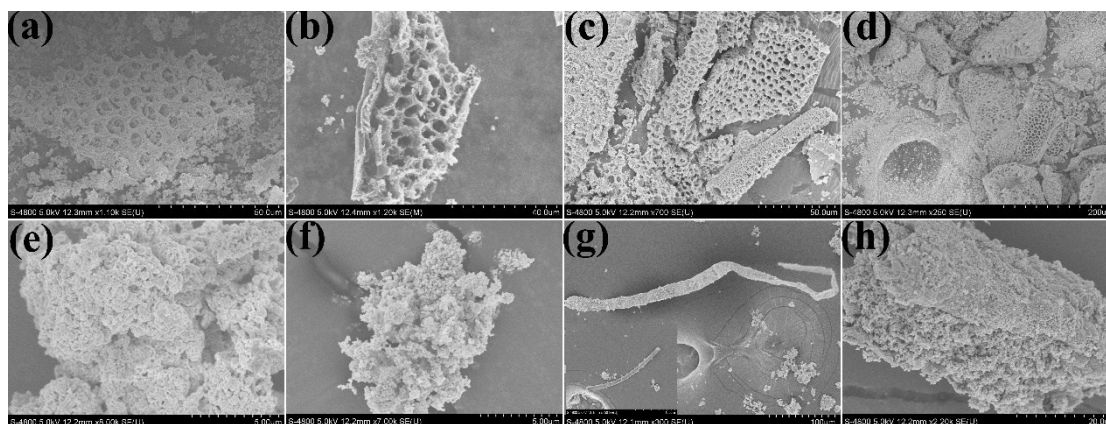


Fig. S1 SEM images of Co-MnO@CN-180 (a), Co-MnO@CN-500 (b), Co-MnO@CN-600 (c), Co-MnO@CN-800 (d), Co-MnO@SiO₂-700 (e), Co-MnO@SBA-15-700 (f), Co-MnO@CNTs-700 (g), and Co-MnO@AC-700 (h).

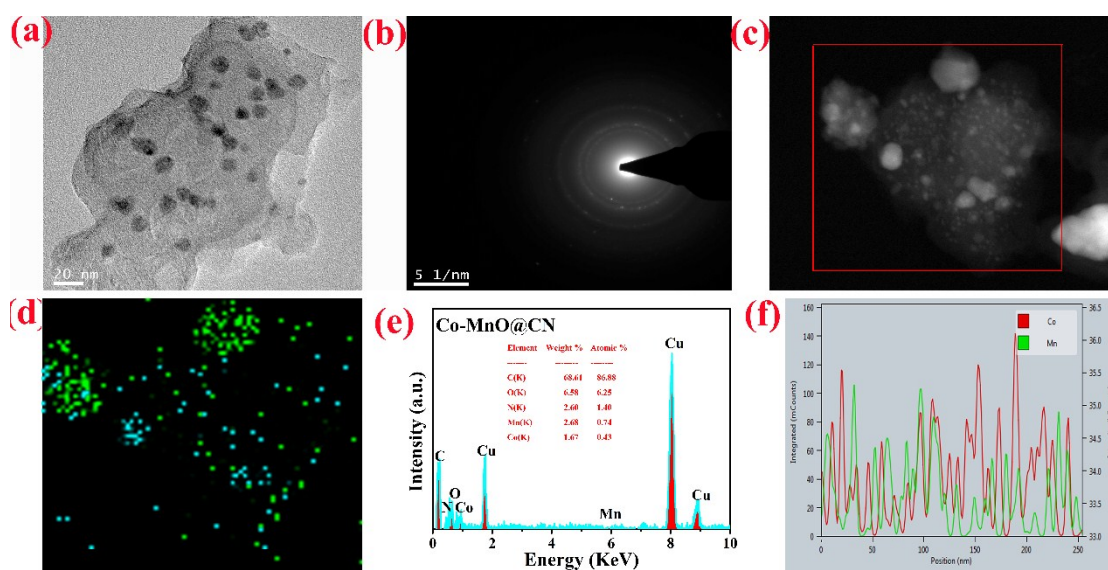


Fig. S2 HRTEM image (a), selected-area diffraction image (b), HAADF-STEM image (c), mapping images of the Co and Mn elements (d), EDS image (e) and line scanning image (f) of Co-MnO@CN-700.

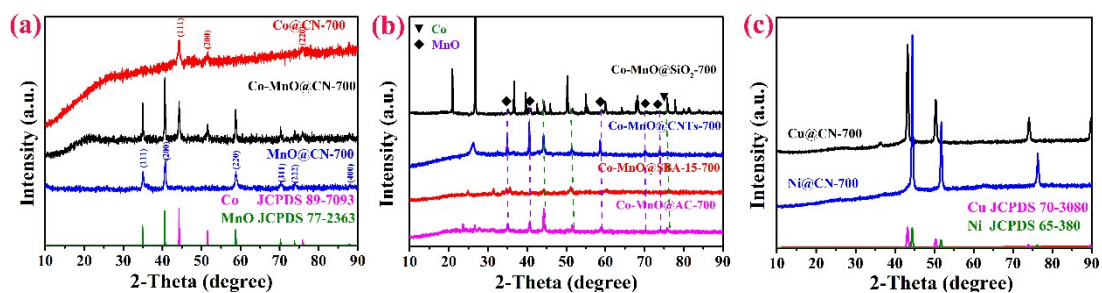


Fig. S3 Comparison of XRD patterns with those of previously reported materials.

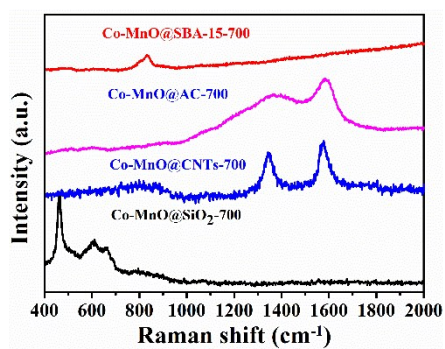


Fig. S4 Comparison of Raman spectra with those of previously reported materials.

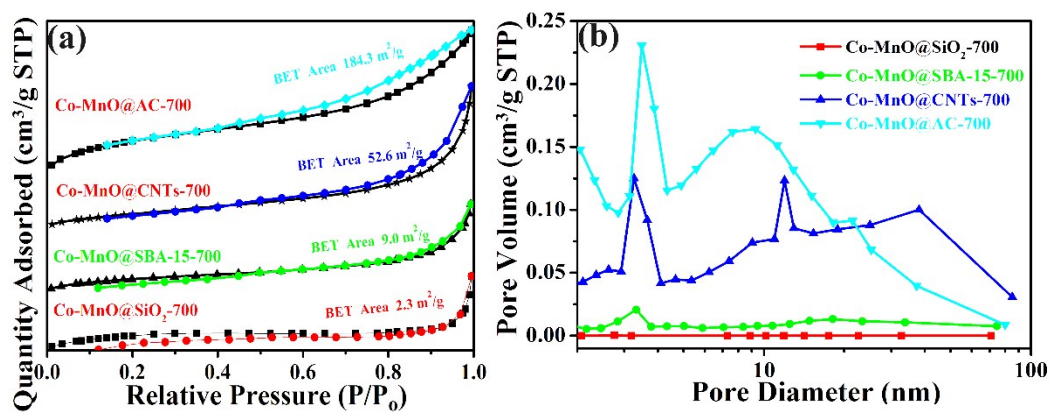


Fig. S5 Comparison of nitrogen adsorption-desorption isotherms with those of previously reported materials.

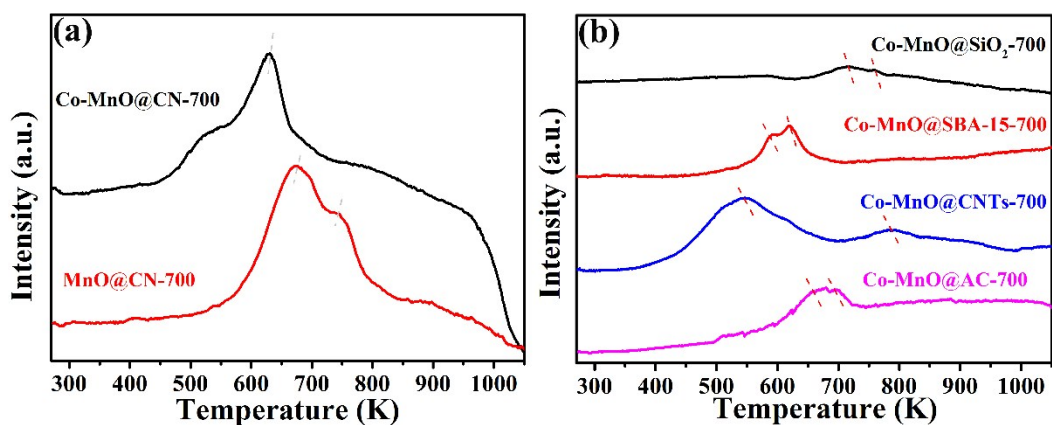


Fig. S6 H_2 -TPR results of as-prepared catalysts.

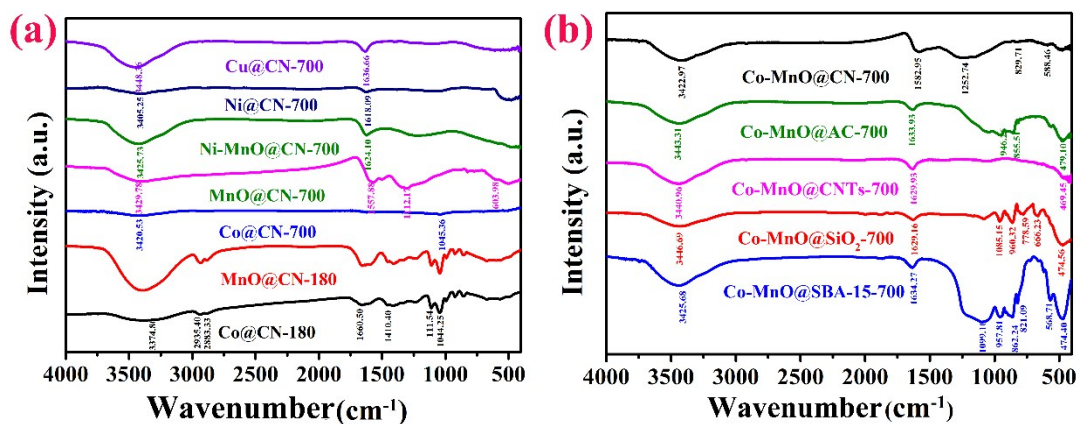


Fig. S7 Comparison of FT-IR spectra with those of previously reported materials.

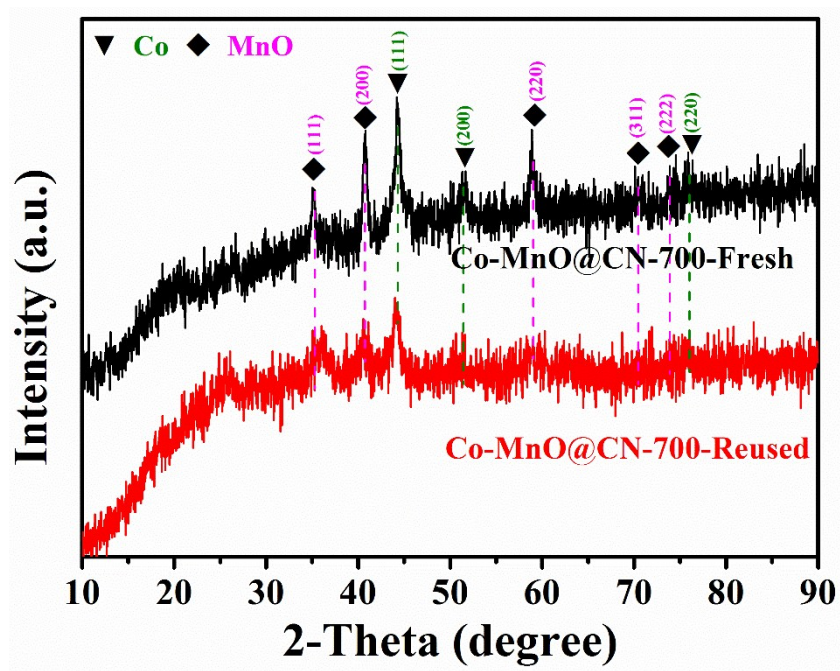


Fig. S8 XRD pattern of reused material.

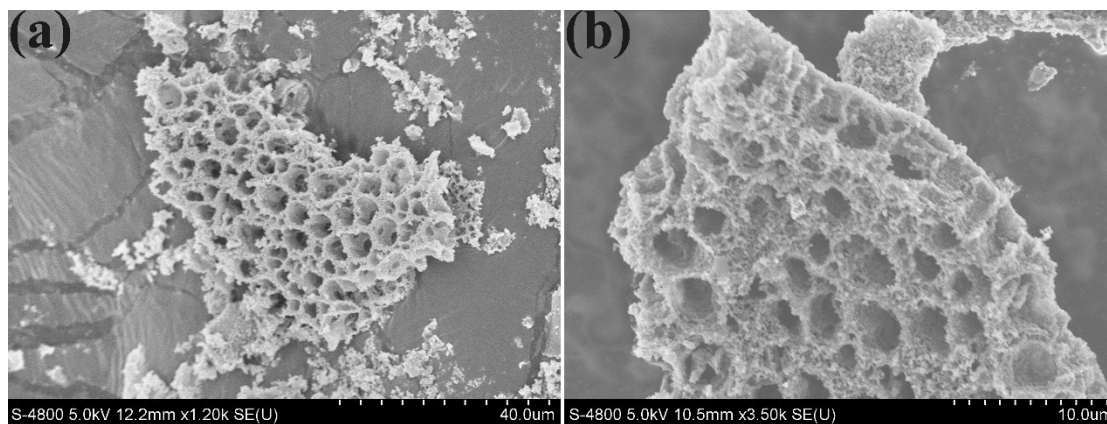


Fig. S9 SEM images of reused material.

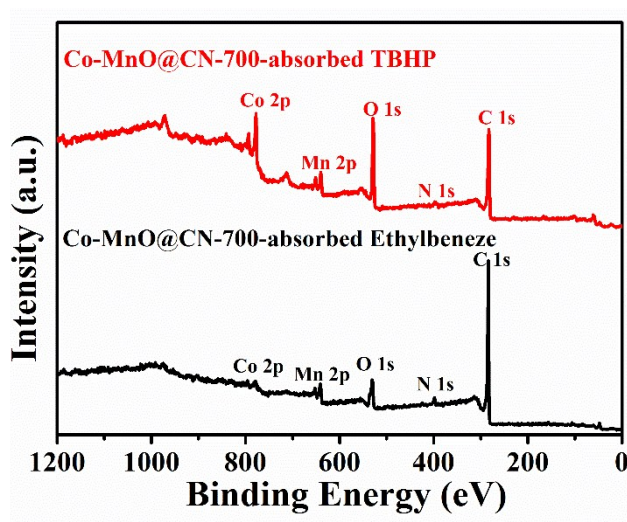


Fig. S10 The wide-scan XPS of material adsorbed with TBHP and ethylbenzene.

References

- [1] T. Liu, H. Cheng, L. Sun, F. Liang, C. Zhang, Z. Ying, W. Lin, F. Zhao, Synthesis of acetophenone from aerobic catalytic oxidation of ethylbenzene over Ti–Zr–Co alloy catalyst: Influence of annealing conditions, *Appl. Catal. A-Gen.*, 512 (2016) 9-14. DOI: 10.1016/j.apcata.2015.12.008
- [2] M. Arshadi, M. Ghiaci, Highly efficient solvent free oxidation of ethylbenzene using some recyclable catalysts: The role of linker in competency of manganese nanocatalysts, *Appl. Catal. A-Gen.*, 399 (2011) 75-86. DOI: 10.1016/j.apcata.2011.03.043
- [3] D. Habibi, A.R. Faraji, M. Arshadi, J.L.G. Fierro, Characterization and catalytic activity of a novel Fe nano-catalyst as efficient heterogeneous catalyst for selective oxidation of ethylbenzene, cyclohexene, and benzylalcohol, *J. Mol. Catal. A- Chem.*, 372 (2013) 90-99. DOI: 10.1016/j.molcata.2013.02.014
- [4] S. Dan-Hua, J. Lin-Tao, L. Zhi-Gang, S. Wen-bin, G. Can-cheng, Ethylbenzene oxidation over hybrid metalloporphyrin@silica nanocomposite microspheres, *J. Mol. Catal. A- Chem.*, 379 (2013) 15-20. DOI: 10.1016/j.molcata.2013.07.007
- [5] B. Gutmann, P. Elsner, D. Roberge, C.O. Kappe, Homogeneous Liquid-Phase Oxidation of Ethylbenzene to Acetophenone in Continuous Flow Mode, *ACS Catal.*, 3 (2013) 2669-2676. DOI: 10.1021/cs400571y
- [6] W. Kanjina, W. Trakarnpruk, Mixed metal oxide catalysts for the selective oxidation of ethylbenzene to acetophenone, *Chinese Chemical Letters*, 22 (2011) 401-404. DOI: 10.1016/j.ccllet.2010.10.035
- [7] S.T. Man, C. Ramshaw, K. Scott, J. Clark, D.J. Macquarrie, R. Jachuck, The Effect of Dehydration in the Oxidation of Ethylbenzene to Acetophenone with Supported Catalysts, *Org. Process Res. Dev.*, 5 (2001) 204-210. DOI: 10.1021/op0000632
- [8] M. Arshadi, M. Ghiaci, A. Rahmanian, H. Ghaziaskar, A. Gil, Oxidation of ethylbenzene to acetophenone by a Mn catalyst supported on a modified nanosized SiO₂/Al₂O₃ mixed-oxide in supercritical carbon dioxide, *Appl. Catal. B-Environ.*, 119-120 (2012) 81-90. DOI: 10.1016/j.apcatb.2012.02.019
- [9] Y. Qin, H. Guo, B. Wang, J. Li, R. Gao, P. Qiu, M. Sun, L. Chen, Controllable Sulfur, Nitrogen Co-doped Porous Carbon for Ethylbenzene Oxidation: The Role of Nano-CaCO₃, *Chem. Asian. J.*, 14 (2019) 1535-1540. DOI: 10.1002/asia.201900086
- [10] Z. Wang, A. Guan, M.C. Kung, A. Peng, H.H. Kung, X. Lv, G. Zheng, L. Qian, In situ formed Co clusters in selective oxidation of α -C H bond: Stabilizing effect from reactants, *Mol. Catal.*, 470 (2019) 1-7. DOI: 10.1016/j.mcat.2019.03.016
- [11] M. Ghiaci, F. Molaie, M.E. Sedaghat, N. Dorostkar, Metalloporphyrin covalently bound to silica. Preparation, characterization and catalytic activity in oxidation of ethyl benzene, *Catal. Commun.*, 11 (2010) 694-699. DOI: 10.1016/j.catcom.2010.01.023